Spectropolarimetric diagnostics of photospheric magnetic fields using Si I 10827 Å and Sr I 4607 Å lines

N. Shchukina[1]*, J. Trujillo Bueno*[2]

[1]Main Astronomical Observatory, NASU, Kyiv, Ukraine

[2]Instituto de Astrofisica de Canarias, La Laguna, Spain

Our mysterious Sun: magnetic coupling between solar interior and atmosphere
Tbilisi, Georgia
25-29 September 2017

The subject of my talk:

Inter-network (IN) small-scale (SS) magnetic fields in the quiet solar (QS) photosphere.

Spectropolarimetric diagnostics from the Zeeman effect

Si I 10827 Å

Science objectives:

The spectral region around 10830 Å
is a powerful diagnostic window:
It contains information coming simultaneously
from
the chromospheric structures
(the He I 10830 Å triplet)
&
from
the whole photosphere
(the Si I 10827 Å).

The scientiic interest on the spectral region around 10830 Å has been growing over the last fifteen years thanks to advances in instrumentation for spectropolarimetric solar observations:

- **4-m Daniel K. Inouye Solar Telescope (DKIST, Keil et al., 2011) with the infrared instruments. They will provide unprecedented IR observations on the solar disk, at the limb, and in the corona with the highest spatial resolution one can achieve from the ground**

- **the 4-m European Solar Telescope (EST, Collados et al., 2013)**

- **the 1.5-m GREGOR solar telescope (Denker et al., 2012; Soltau et al., 2012) hosted with IR Spectrograph for spectropolarimetry in the 10 000−18 000 A region; (GRIS, Collados et al., 2012)**

- **the Japanese Aerospace Exploration Agency mission Solar-C (Shimizu et al., 2011; Katsukawa et al., 2012) aimed at high spatial resolution, high cadence IR spectropolarimetric observations**

The circular and linear polarization sensitivity:

$$S_V = g_{eff}\, d_C\, \lambda / \lambda_{ref}$$

$$S_Q = G_{eff}\, d_C (\lambda / \lambda_{ref})^2$$

with g_{eff} the effective Landé factor and

G_{eff} the second order effective Landé factor

$$\lambda_{ref} = \text{FeI } 6302 \;\; g_{eff} = 2.5 \;\; G_{eff} = 6.25 \;\; d_C = 0.65$$

$$\lambda = \text{SiI } 10827 \;\; g_{eff} = 1.5 \;\; G_{eff} = 2.25 \;\; d_C = 0.7$$

$$\boxed{S_V(10827) / S_V(6302) = 1.11}$$

$$\boxed{S_Q(10827) / S_Q(6302) = 1.14}$$

See **Landi degl´Innocenti & Landolfi (2004): eq. (9.88) & eq. (9.89)**

Such unprecedented facilities for doing solar IR spectropolarimetric observations requires further development of diagnostic tools.

Zeemen diagnostics: methods

- Magnitograph-like analysis based on the weak field approximation
- The bisector and the center-to-gravity techniques
- Inversion techniques (SIR, NICOLE codes)
- Line ratio techniques
- MHD modelling & comparison with observations

Zeeman diagnostics:

Weak field approximation

deduces some properties of the solutions to the transfer equations for polarization radiation (Stokes Q, U, V) without actually solving them

Weak field approximation

Two assumptions:

1. Zeeman splitting is smaller than the line width of the intensity *I* profile:

$$g_{eff} \frac{\Delta\lambda_B}{\Delta\lambda_D} << 1$$

2. The longitudinal *B^L=B·cosθ* and transverse *B^T=B·sinθ* components of the field, the azimuth χ, the line of sight velocity ω_A are independent of optical depth

$$V(\lambda) = -\Delta\lambda_B g_{eff} \cos\Theta \frac{\partial I}{\partial\lambda} \qquad \Delta\lambda_B = 4.668 \cdot 10^{-10} \lambda^2 B$$

$$\sqrt{\{Q^2(\lambda) + U^2(\lambda)\}} = \frac{3}{4} \cdot \Delta\lambda_B^2 \cdot G_{eff} \sin^2\Theta \frac{1}{(\lambda_W - \lambda_0)} \cdot \frac{\partial I}{\partial\lambda}$$

Key question:

Is the weak field approximation valid for the Si I 10827 Å line formed in the real solar atmosphere?

To answer this question

1. We calculate Stokes profiles in the model atmosphere with non-negligible surface and height variations of the

- **velocity field;**
- **magnetic field;**
- **thermodynamic parameters (density, temperature).**

2. We apply the weak field approximation to the calculated Stokes I, Q, U, V supposing that they represent “REAL Sun” observations.

3. We compare recovered longitudinal and transverse components of the magnetic field with the “REAL field”.

We use

Magneto-convection simulation with small-scale dynamo (SSD) action.

A vertical unsigned flux density $< |B_z| > = 80$ G in the visible surface layers & zero net magnetic flux.

(M.Rempel, 2014, ApJ, 789, p.132)

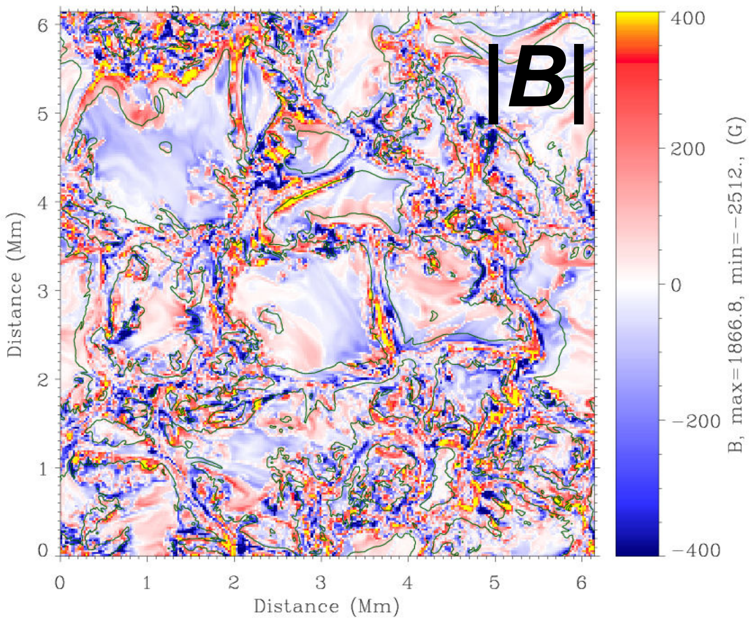

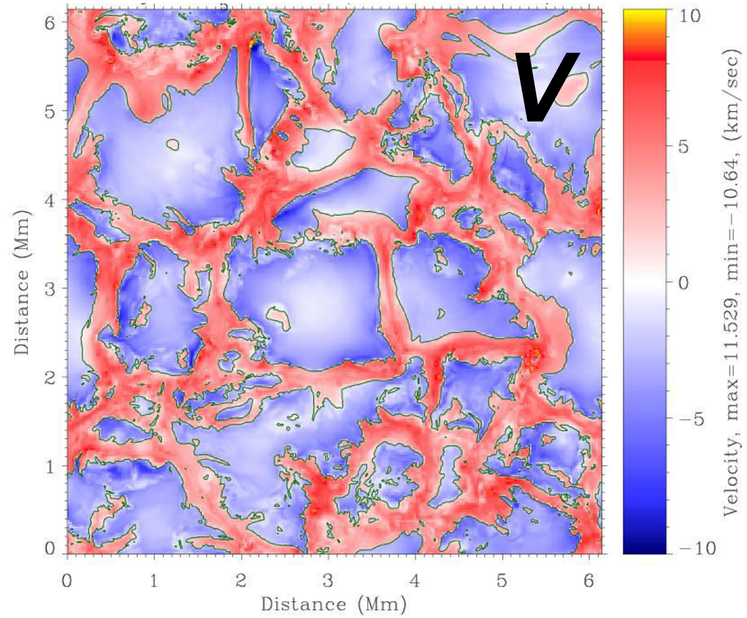

Surface variations of the modulus *B* (with *Bz* sign), velocity *V* & temperature *T* at continuum level

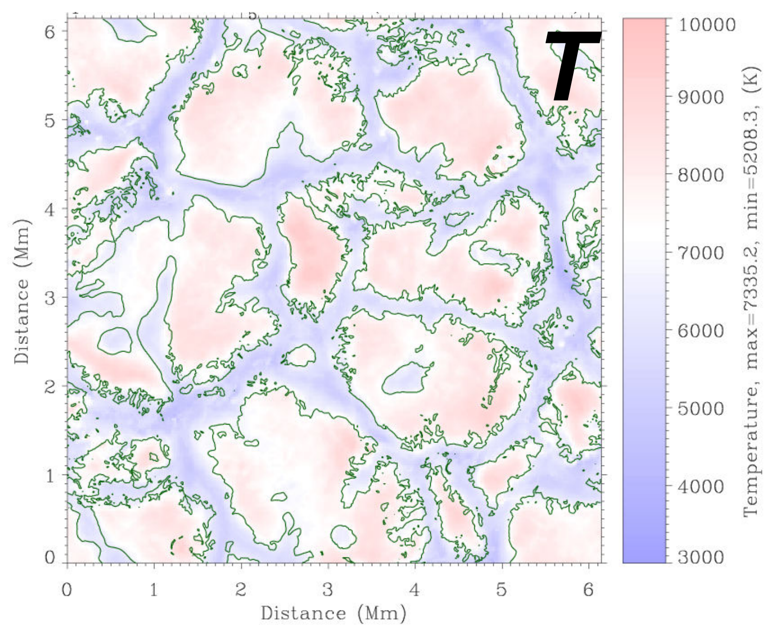

Verical variations of the modulus field strength IBI (with Bz sign) in MHD 3D snapshot

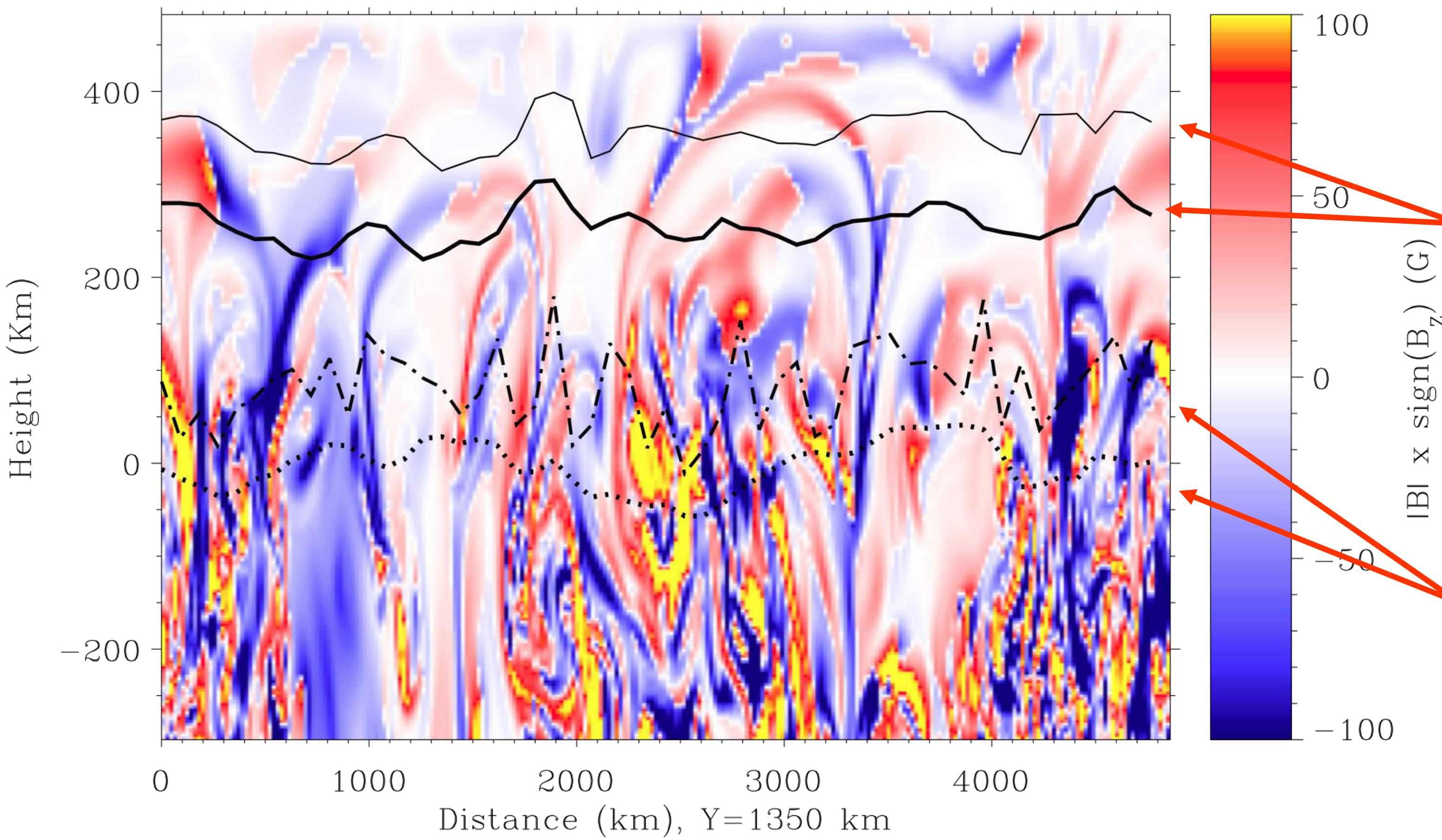

Region of "formation" of the Si I 10827 **ZEEMAN** signals

Region of "formation" of the Fe I 6302 **ZEEMAN** signals

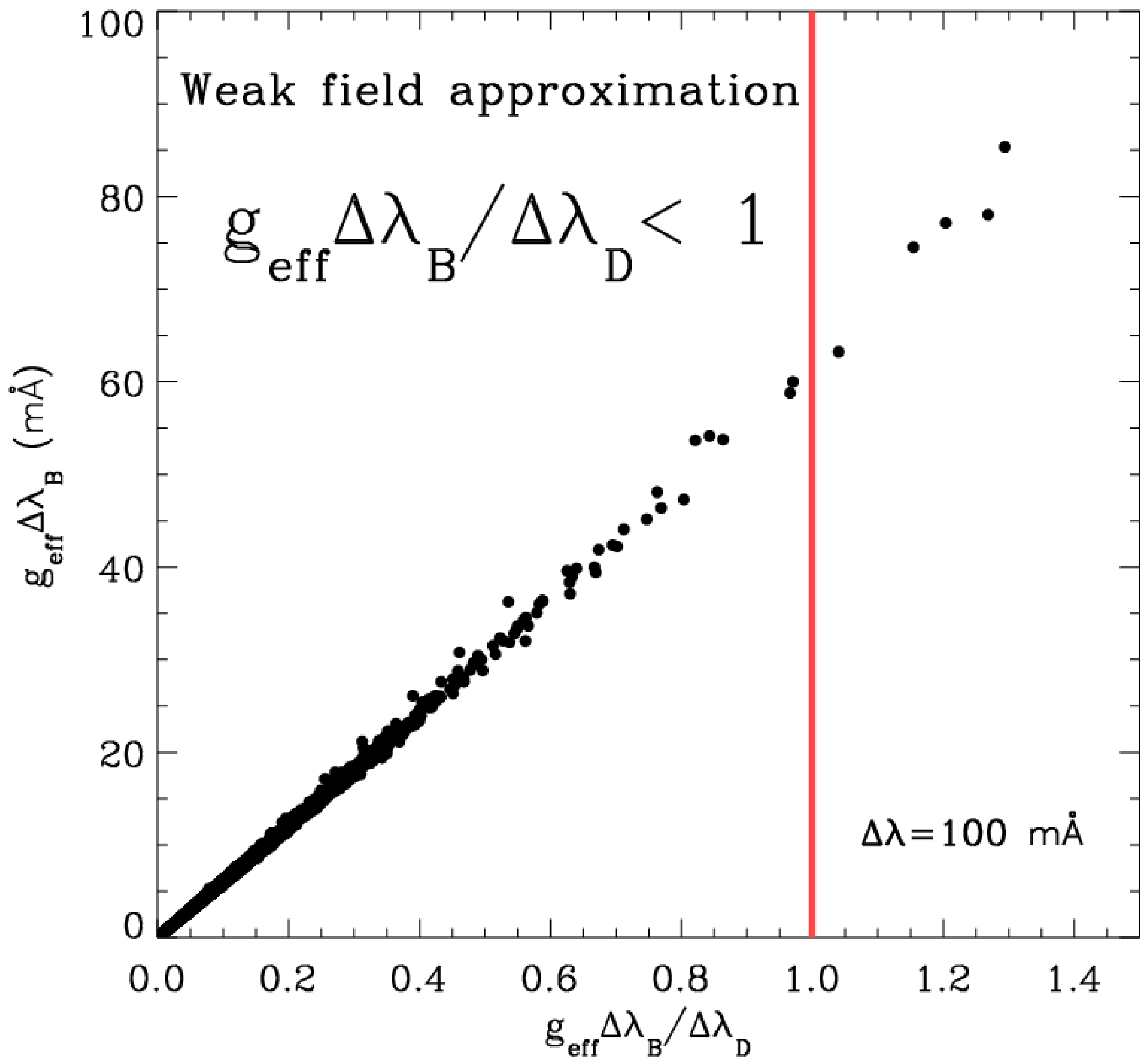

In the 3D Rempel's snapshot Zeeman splitting is smaller than the line width of the intensity *I* profile

NLTE modelling

We solved the self-consistent statistical and radiative transfer equations applying our multilevel transfer code (Shchukina & Trujillo Bueno, 2001; Shchukina et al. 2017).

It allows to compute the NLTE Stokes *I, Q, U, V* parameters of spectral lines by taking the Zeeman effect into account.

Key point:

For the Si I 10827 Å Stokes profiles *I, Q, U, V* formed in the real solar atmosphere the NLTE effects are important

See details in Shchukina, Sukhorukov, Trujillo Bueno, 2017, A&A, 603, A98

Synthesized Stokes profiles

(noise-free unsmeared case

solar disk center)

Typical examples of intergranular (left panel) and granular (right panel) Si I 10827 intensity profiles

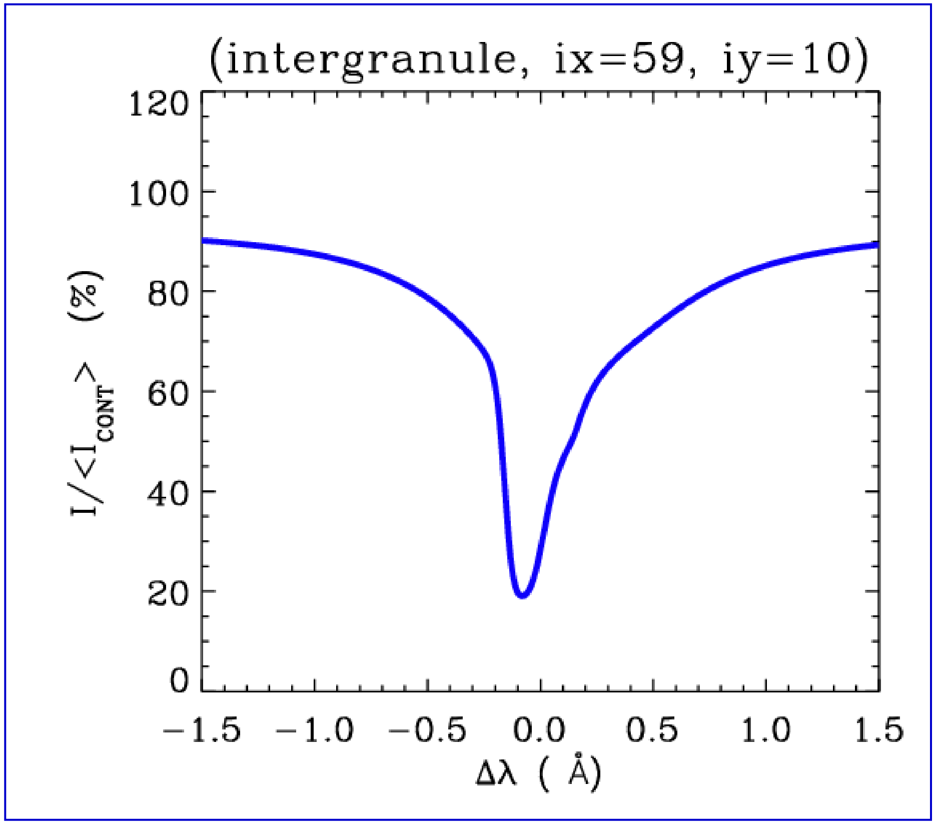

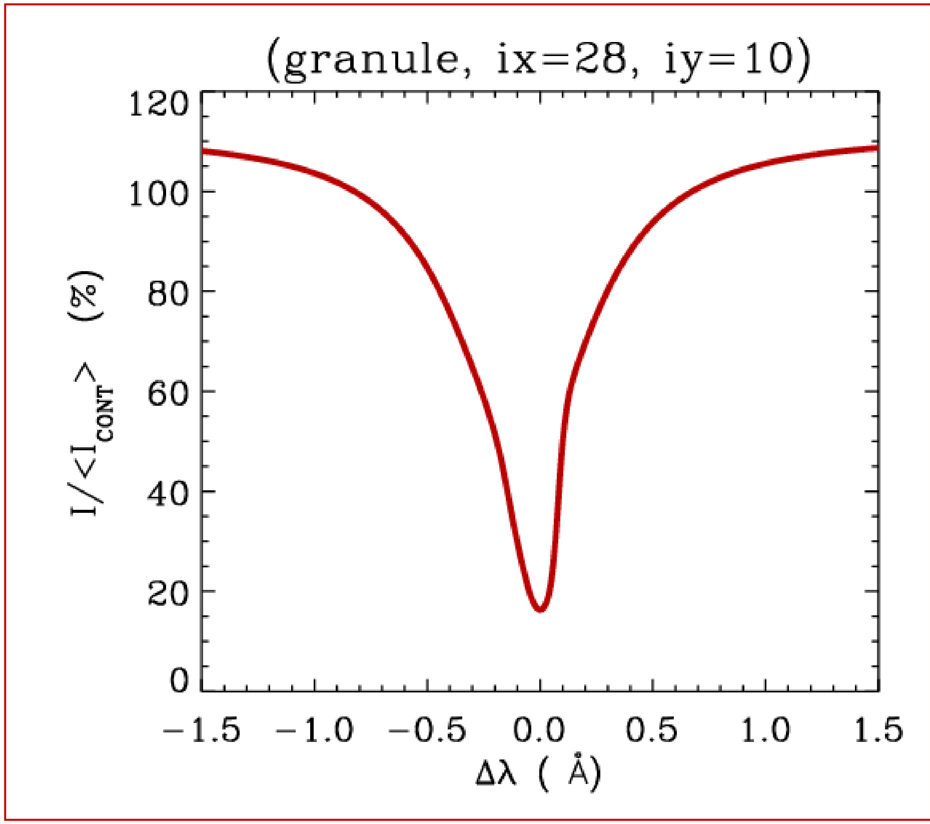

The intensity profiles are very different due to different thermodynamical parameters (*T, P, V*) of the granular and intergranular atmosphere

Typical examples of intergranular (left panel) and granular (right panel) Stokes *V* Si I 10827 line profiles

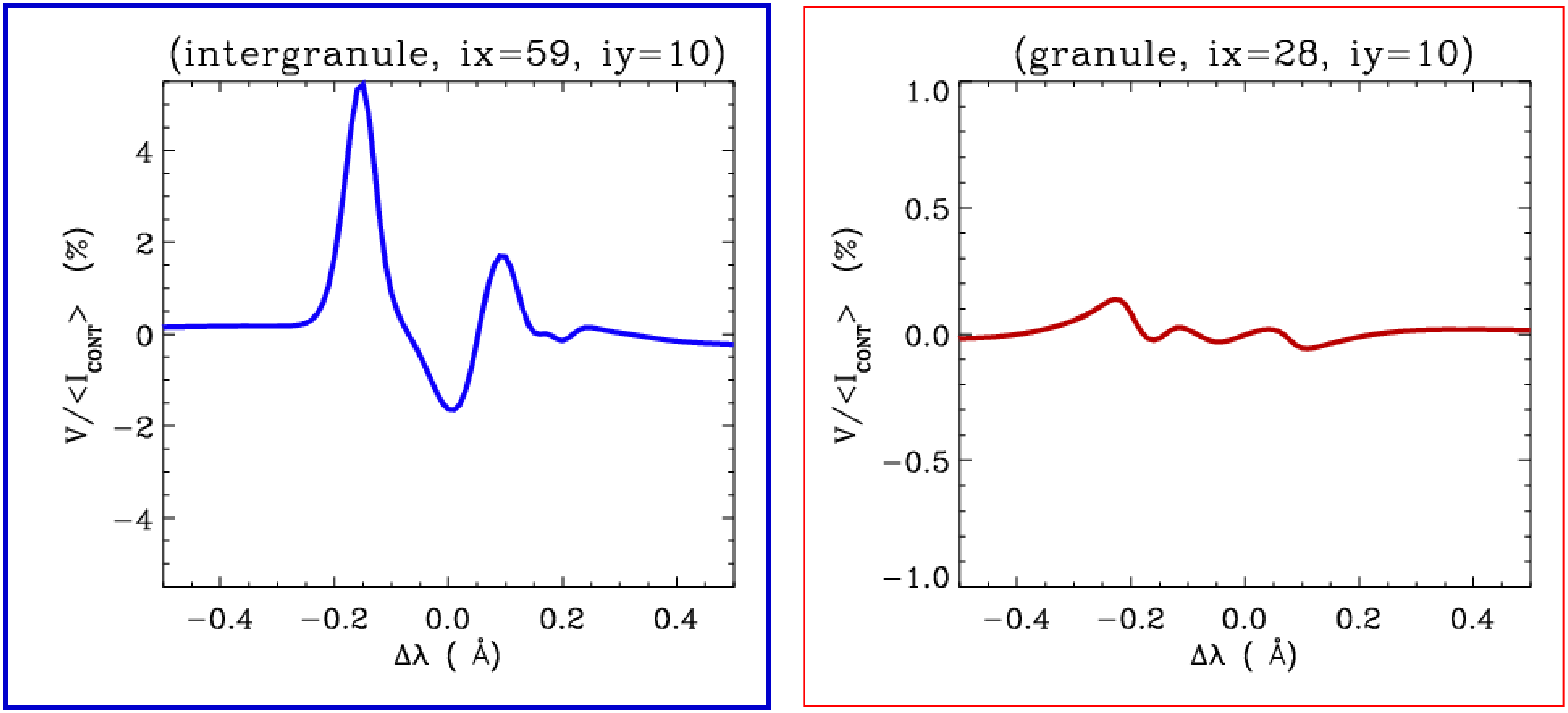

The circularly (and linearly) polarized line profiles have irregular shape due to the changes of the magnetic field along the line-of sight in the presence of velocity gradient (Khomenko et al. 2005)

The ubiquitous presence of Zeeman-like signatures in the Stokes *V*, *Q*, *U* Si I 10827 Å profiles

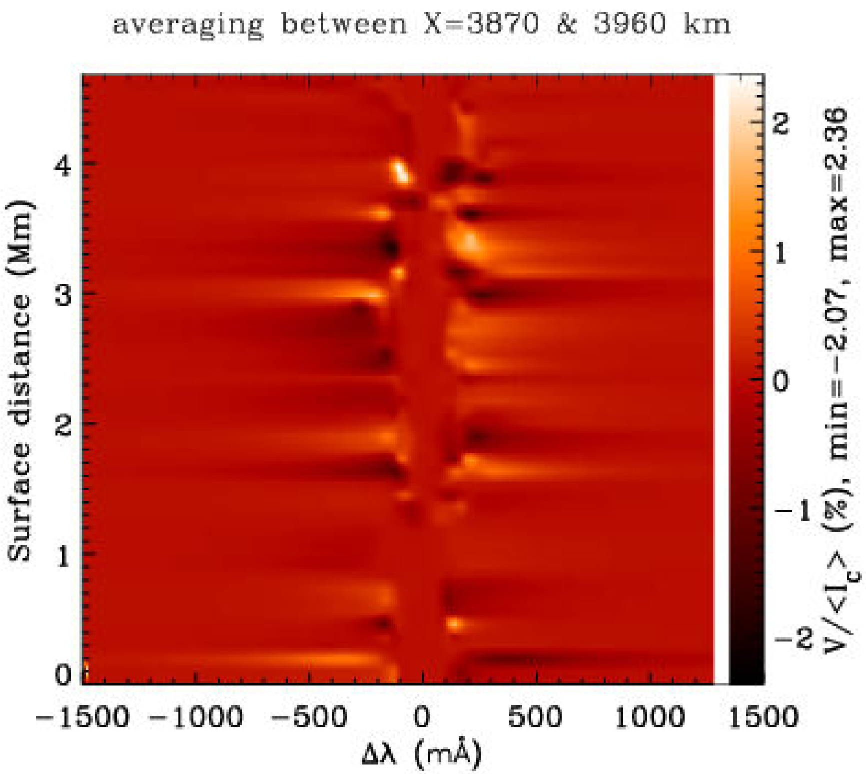

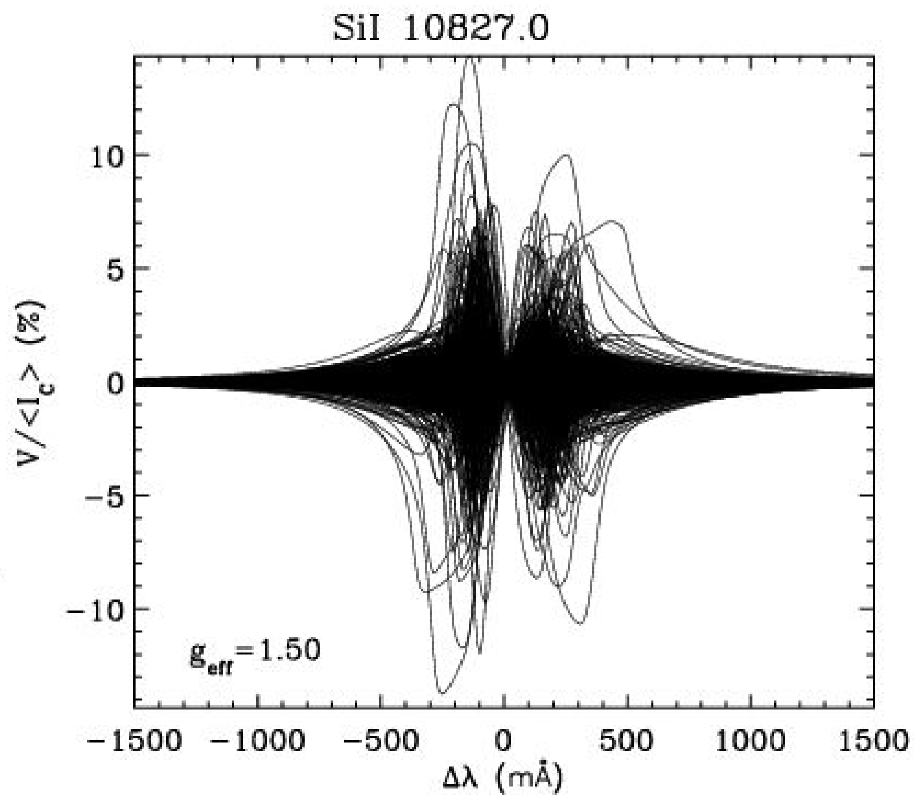

Disk-center Stokes profiles *V* measured in units of spatially averaged mean continuum <*Icont*> .

LEFT: **The wavelength variation of the *V/<Icont>* along the spectrograph's slit.**

RIGHT: **The spatially resolved emergent *V/<Icont>* profiles at each of the surface grid points.**

Sensitivity of the polarization signals in the Si I 10827 line to the intensity derivative

noise-free unsmeared case
solar disk center

Typical examples of intergranular (left panel) and granular (right panel) Si I 10827 intensity derivatives

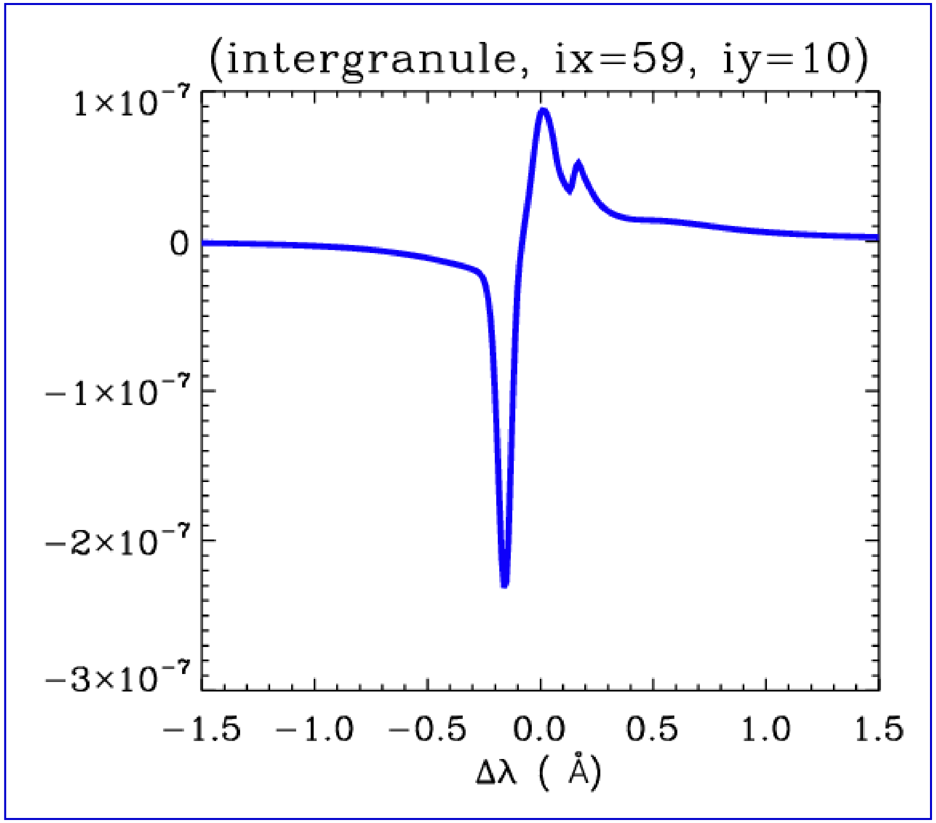

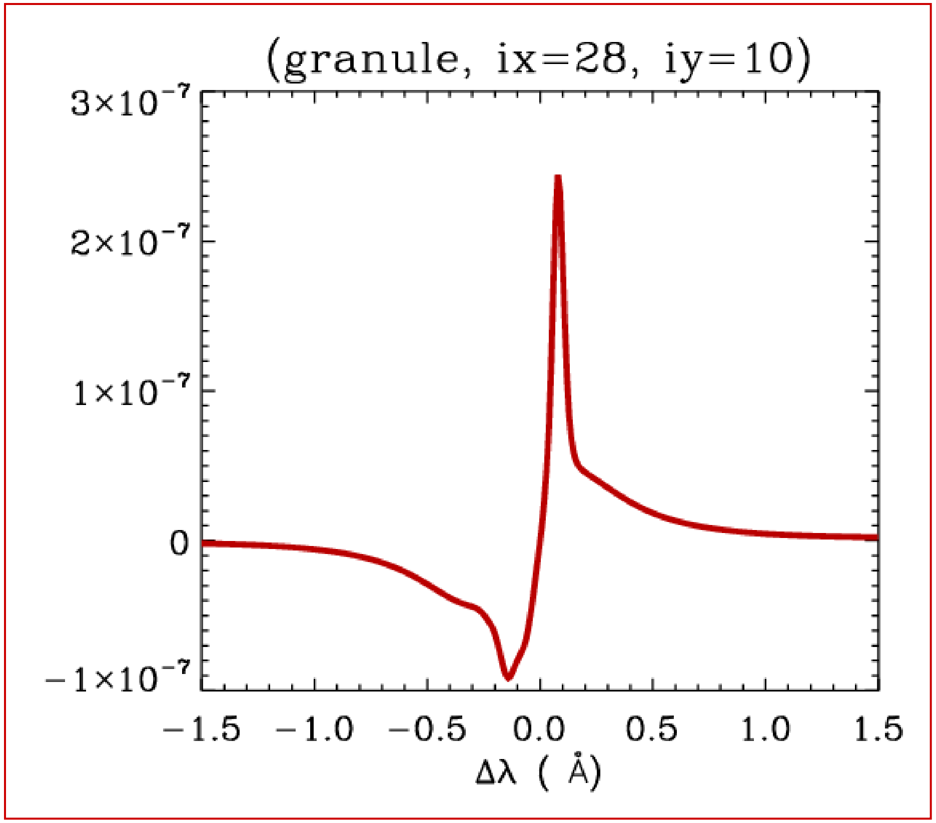

The Stokes V polarization signal in the red wing of the Si I 10827 line VS the intensity derivative taken at

$$\Delta\lambda = 100 \text{ mÅ}$$

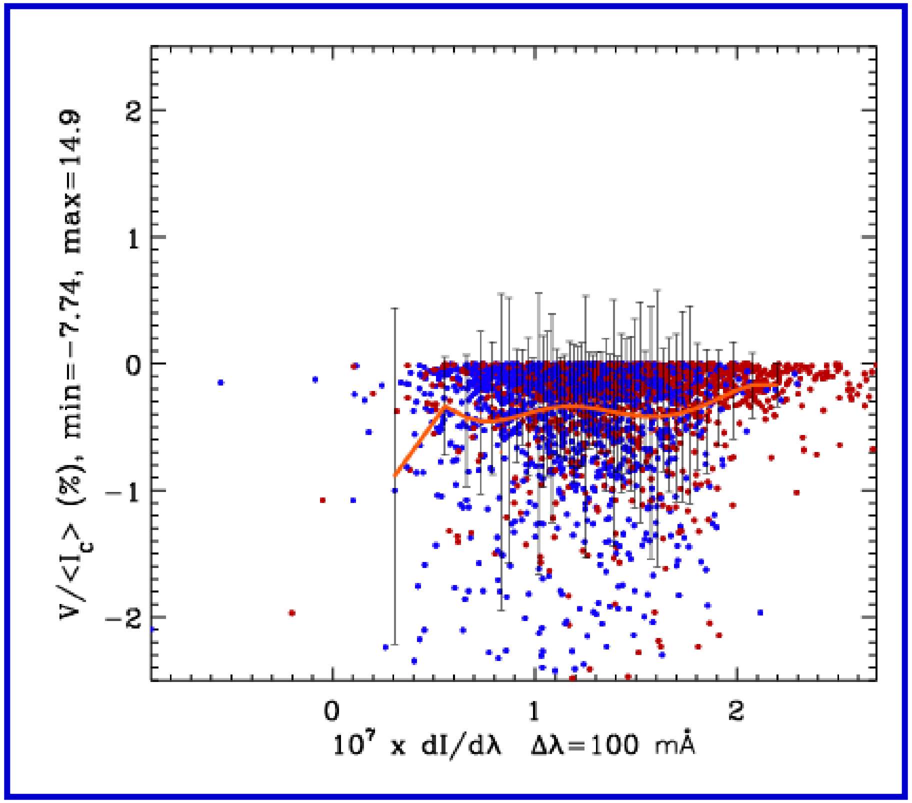

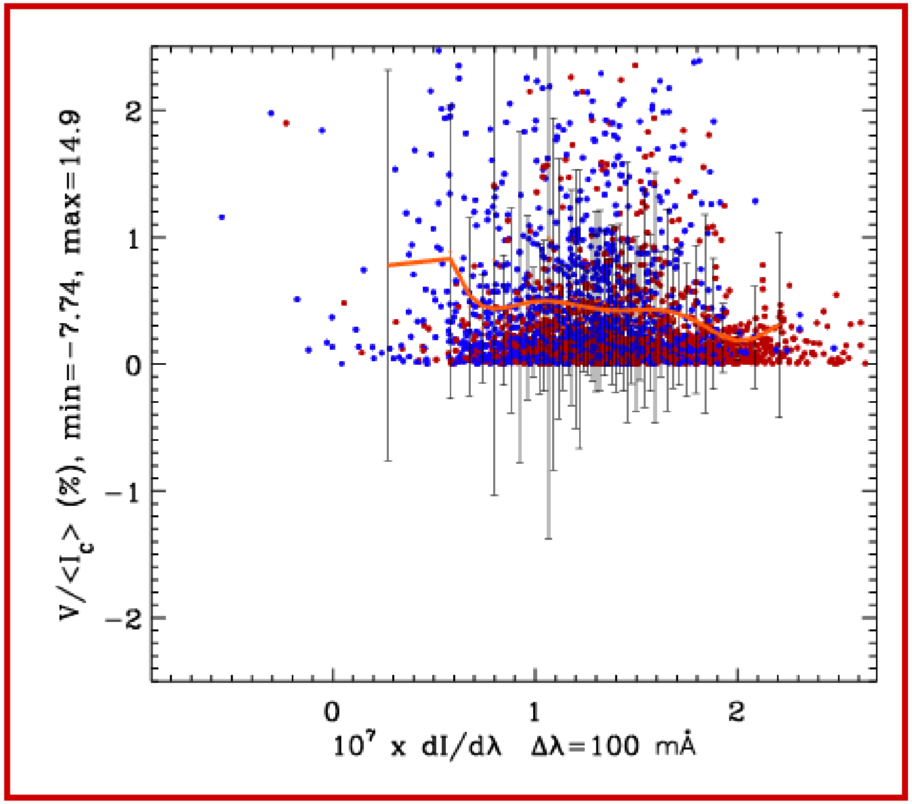

Sensitivity of the polarization signals in the Si I 10827 line to the magnetic field

noise-free unsmeared case
solar disk center

The circular polarization signal in the blue and red wings of the Si I 10827 line versus the LONGITUDINAL component of magnetic field

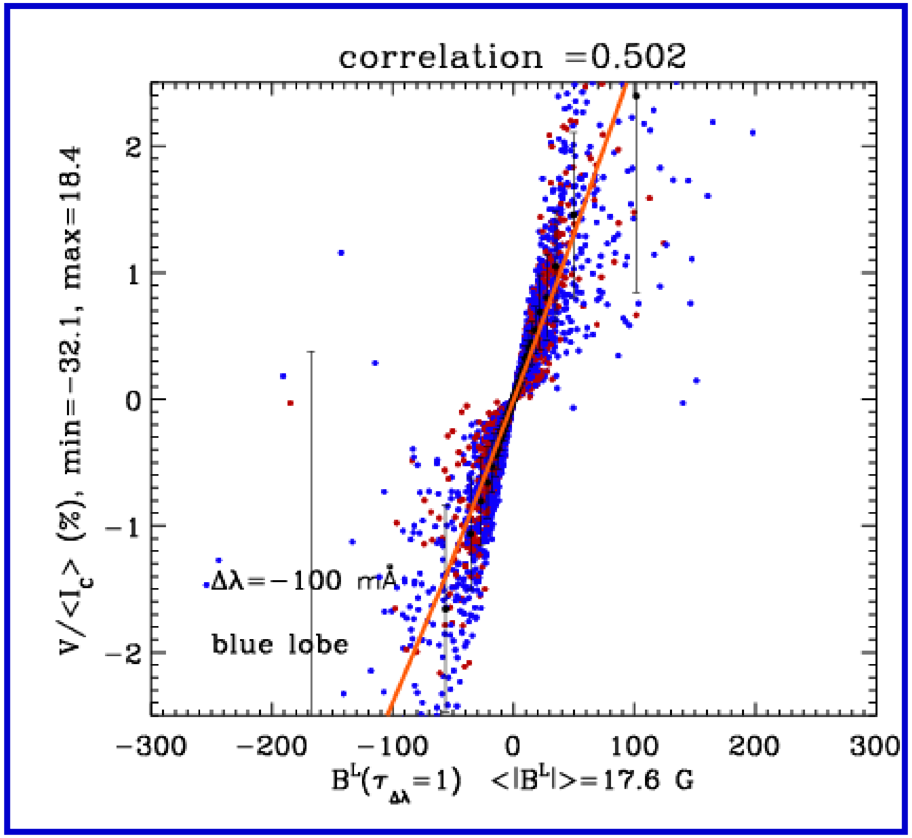

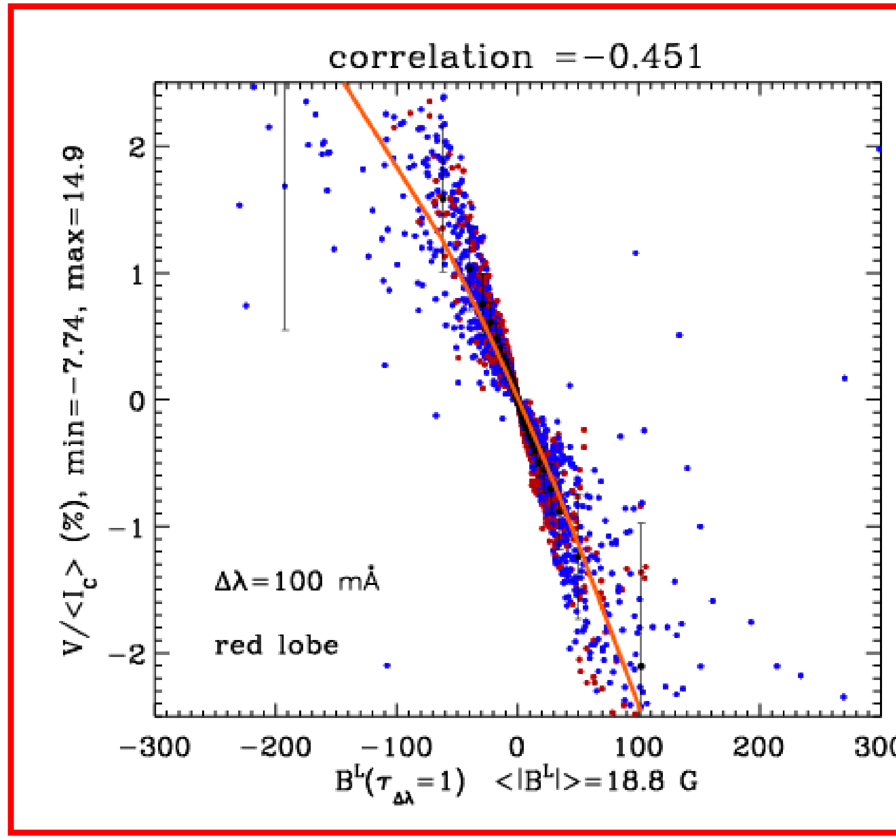

$\Delta\lambda = -100$ mÅ

$\Delta\lambda = 100$ mÅ

The linear polarization signal in the blue and red wings of the Si I 10827 line versus the TRANSVERSE component of magnetic field

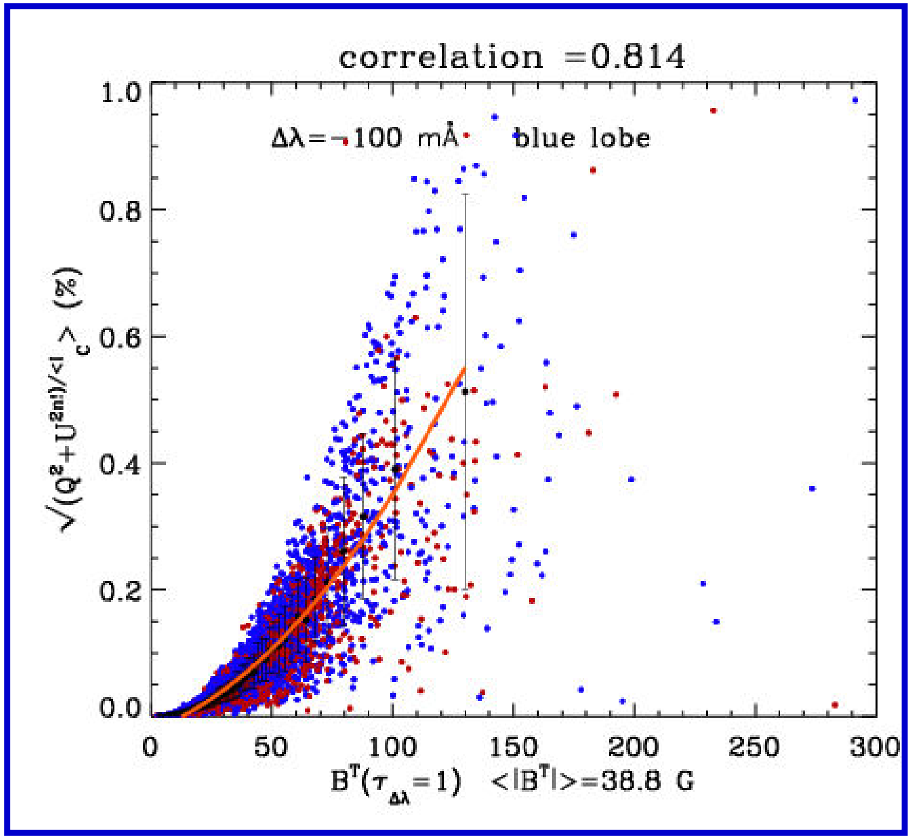

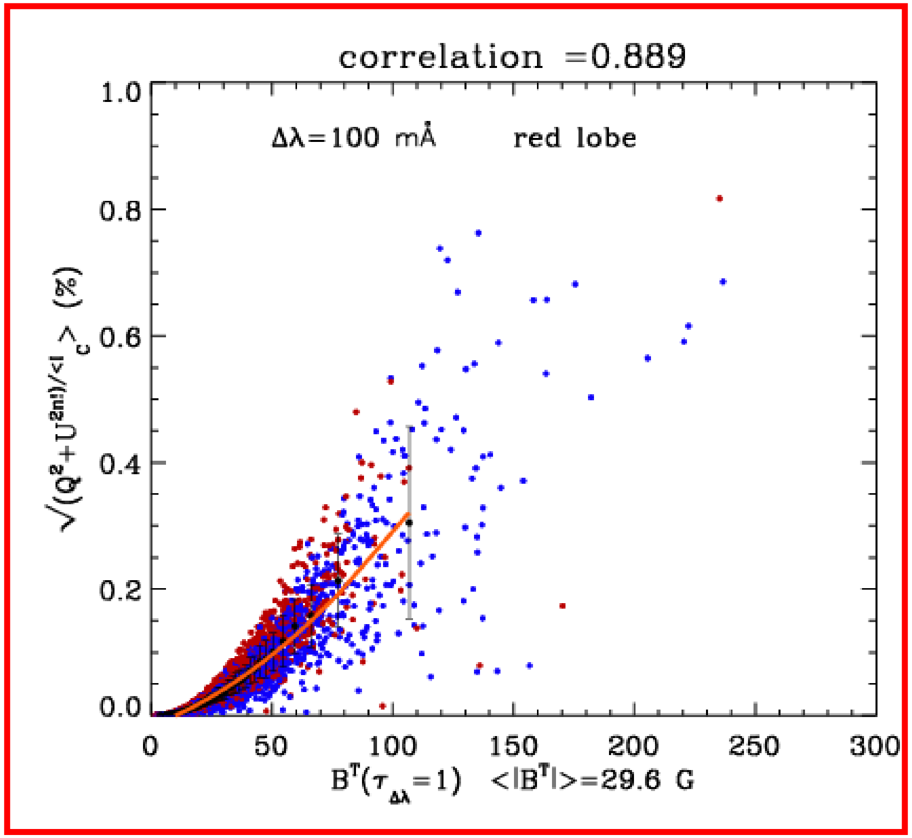

$\Delta\lambda = -100$ mÅ

$\Delta\lambda = 100$ mÅ

Magnetic field recovered

(noise-free unsmeared case

solar disk center)

Height of formation of the Si I 10827 Å

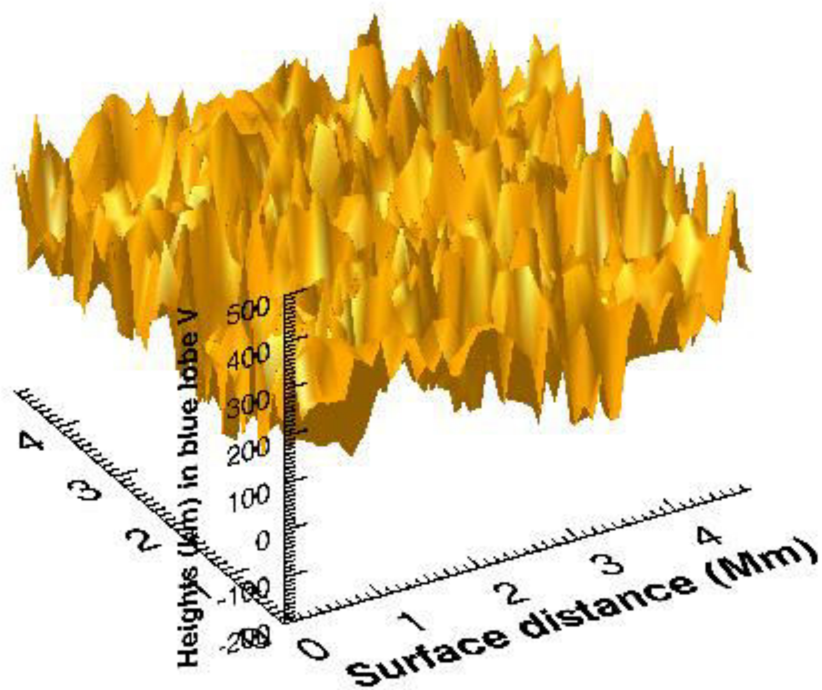

Eddington-Barbier approximation: heights where $\tau_{\Delta\lambda}=1$

The longitudinal component of the magnetic field recovered from the blue and red wings of the Si I 10827 line VS the "real" verical magnetic field B_Z taken at the heights, where the NLTE optical depth at given wavelength $\tau_{\Delta\lambda} = 1$

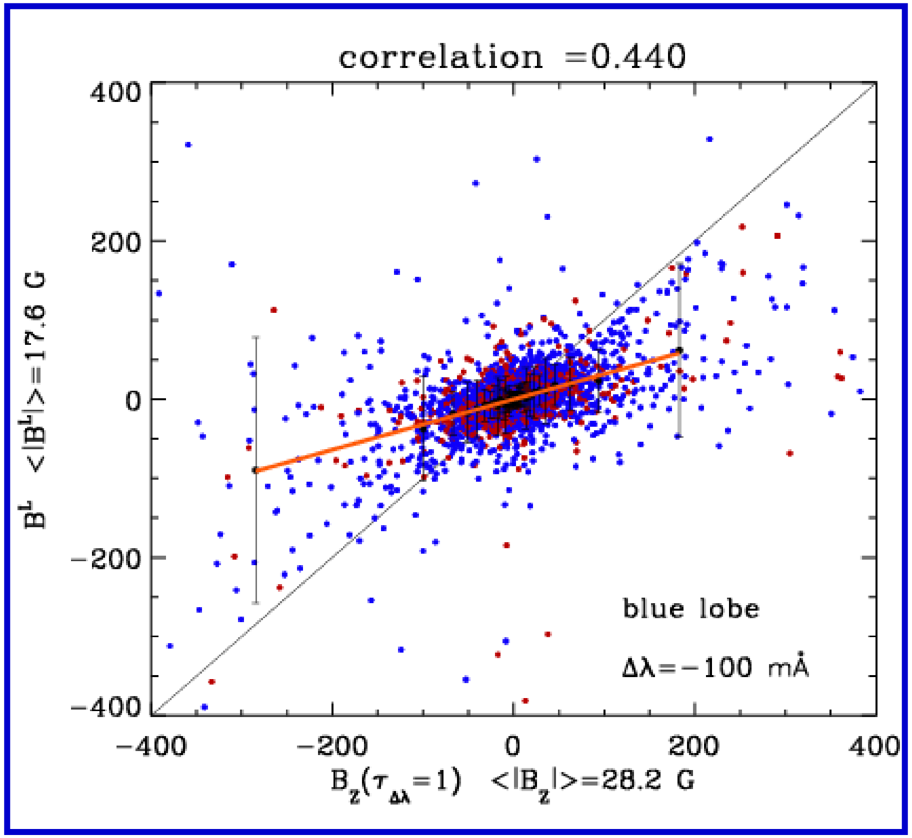

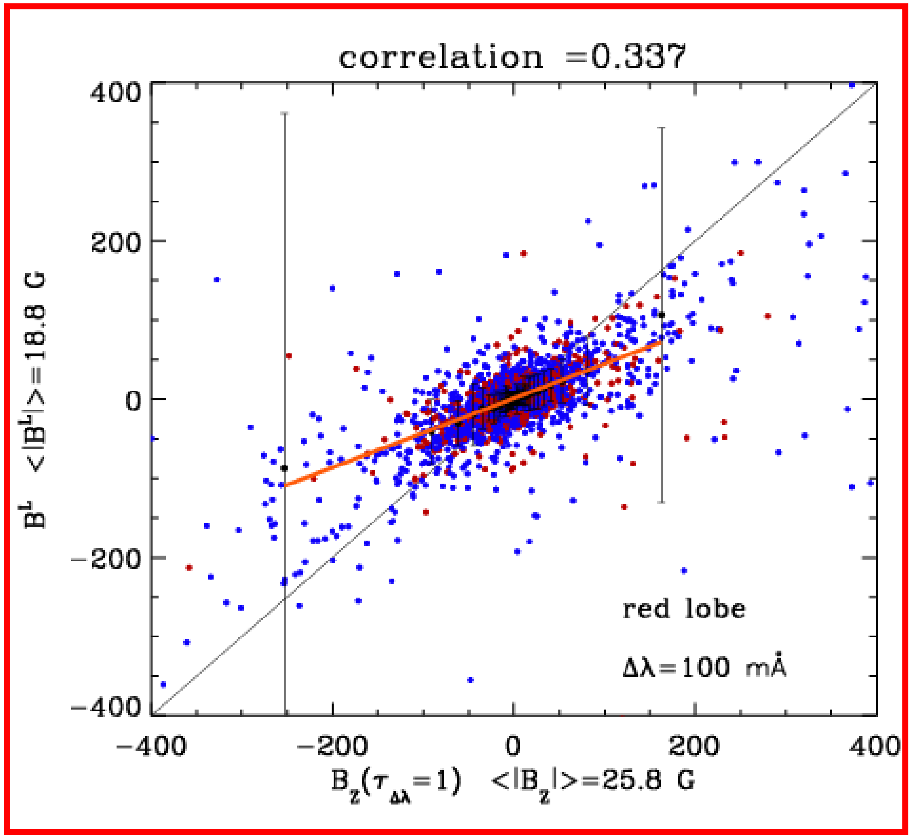

$\Delta\lambda = -100$ mÅ

$\Delta\lambda = 100$ mÅ

The transverse component of the magnetic field recovered from the blue and red wings of the Si I 10827 line VS the "real" verical magnetic field B_Z taken at the heights, where the NLTE optical depth at given wavelength $\tau_{\Delta\lambda}=1$

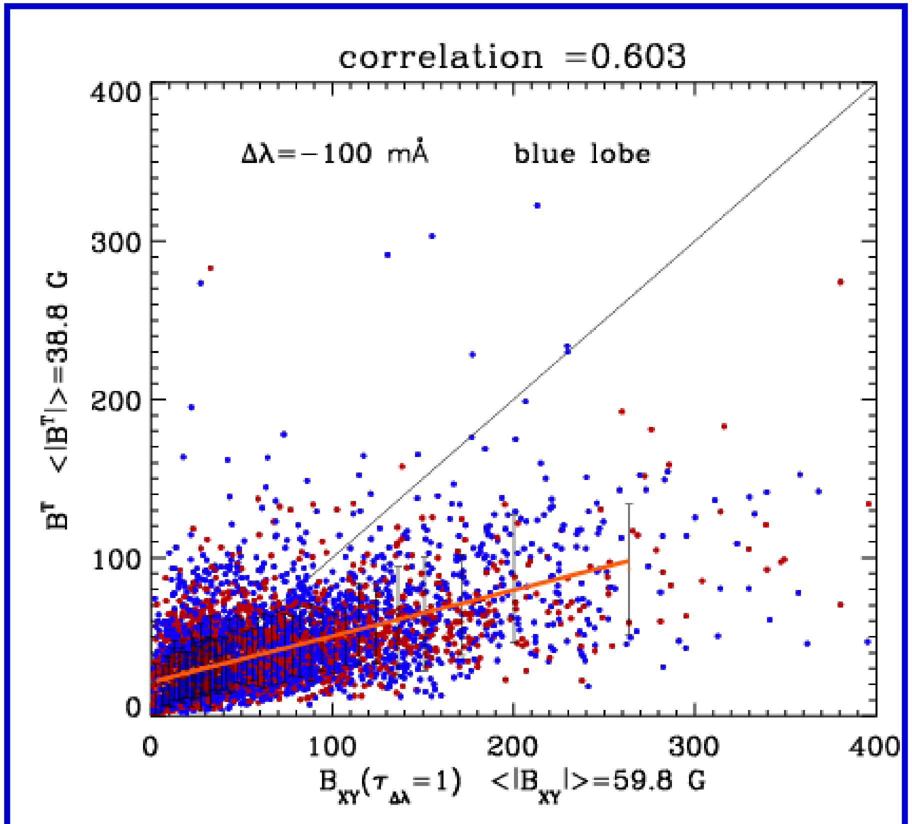

$\Delta\lambda=-100$ mÅ

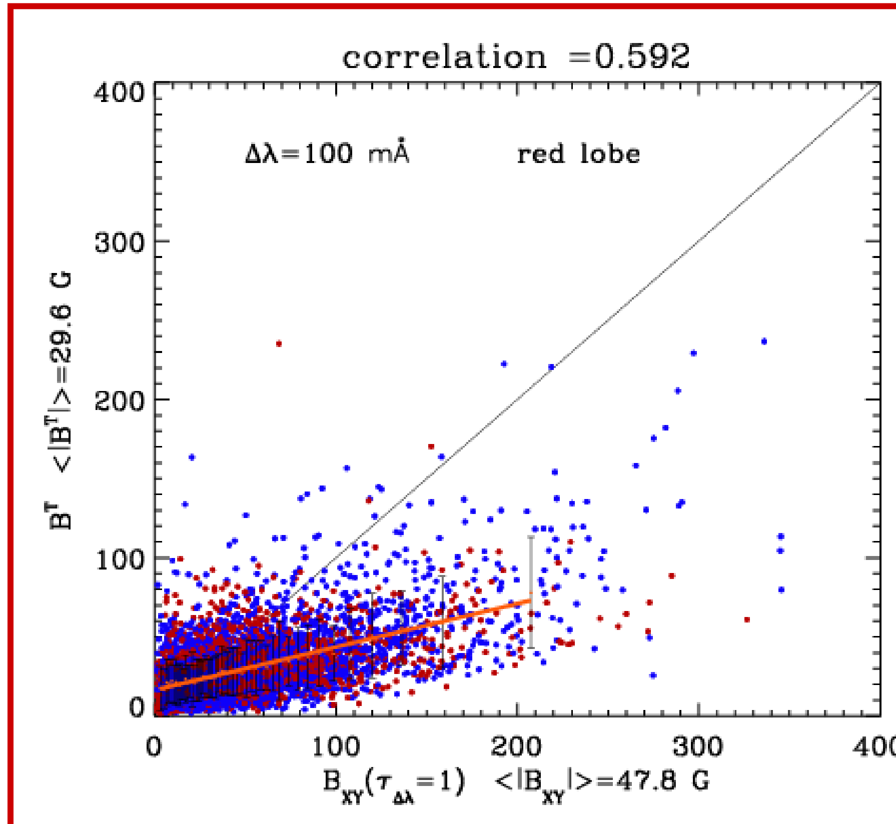

$\Delta\lambda=100$ mÅ

Probability Distribution Functions (PDF)

(noise-free unsmeared case

solar disk center)

$$\Delta\lambda = \pm 100$$ **mÅ**

Red line: PDF for the LONGITUDINAL component of the magnetic field obtained from the blue (left) and red (right) wings.

Dashed line: PDF for the "real" vertical magnetic field taken at the surface $\tau_{\Delta\lambda} = 1$

Solid line: the "real magnetic field" taken at the fixed height = mean height <H> of formation of the layer $\tau_{\Delta\lambda} = 1$

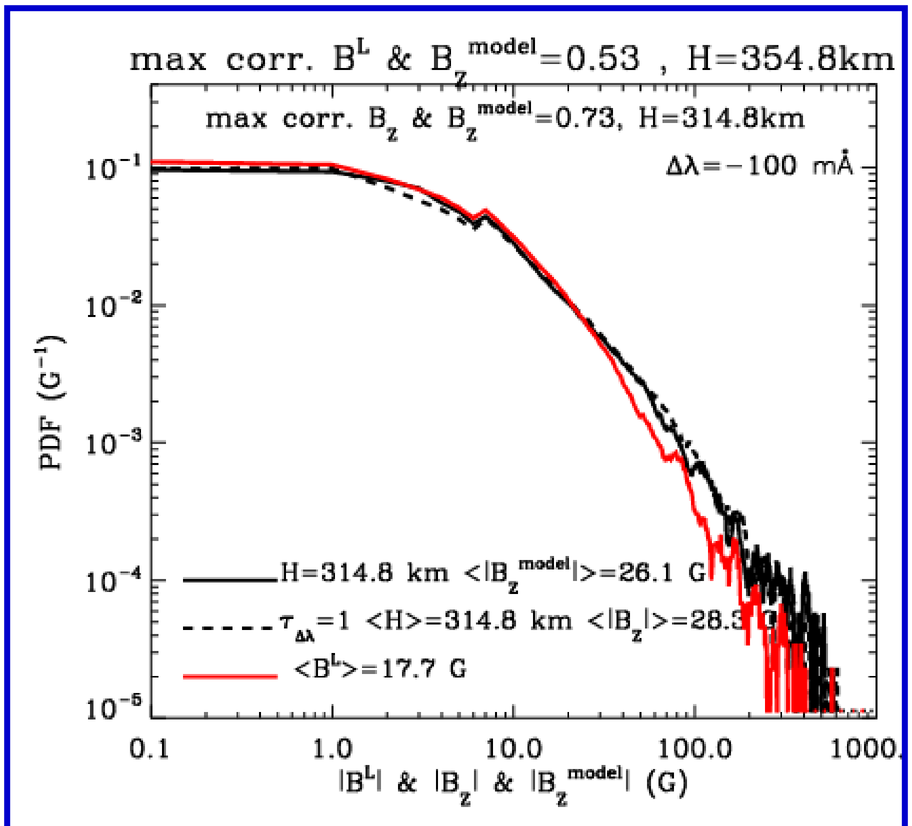

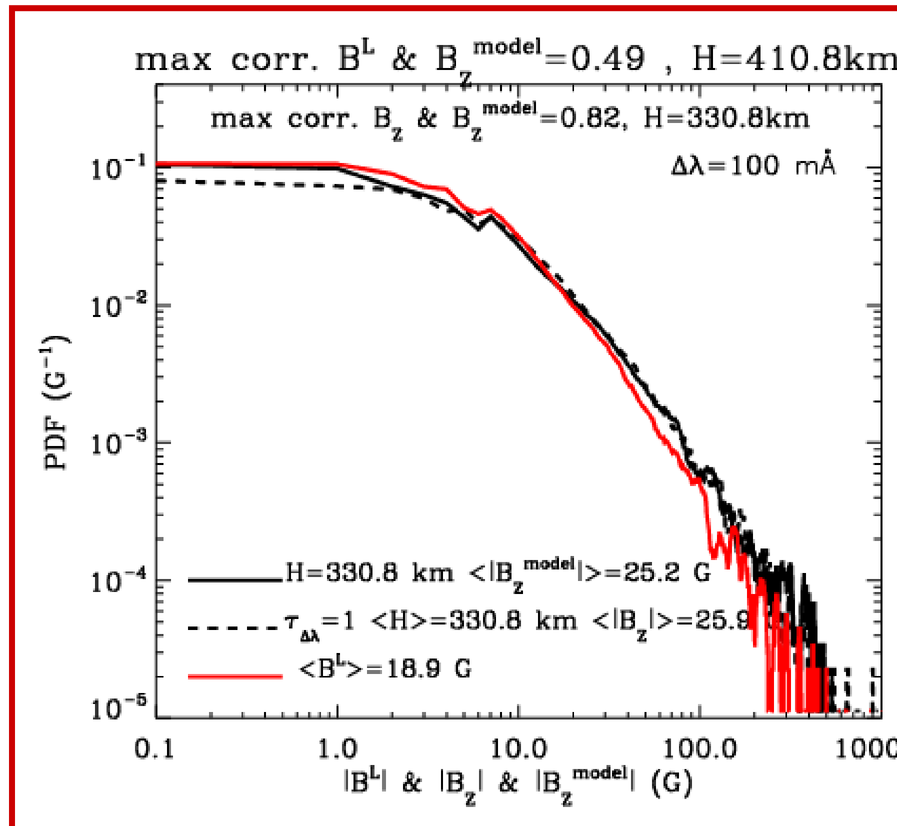

Red line: PDF for the **TRANSVERSE** component of the magnetic field obtained from the blue and red wings.

Dashed line: PDF for the "real" vertical magnetic field taken at the surface $\tau_{\Delta\lambda} = 1$

Solid line: the "real magnetic field" taken at the fixed height = mean height <H> of the layer $\tau_{\Delta\lambda} = 1$

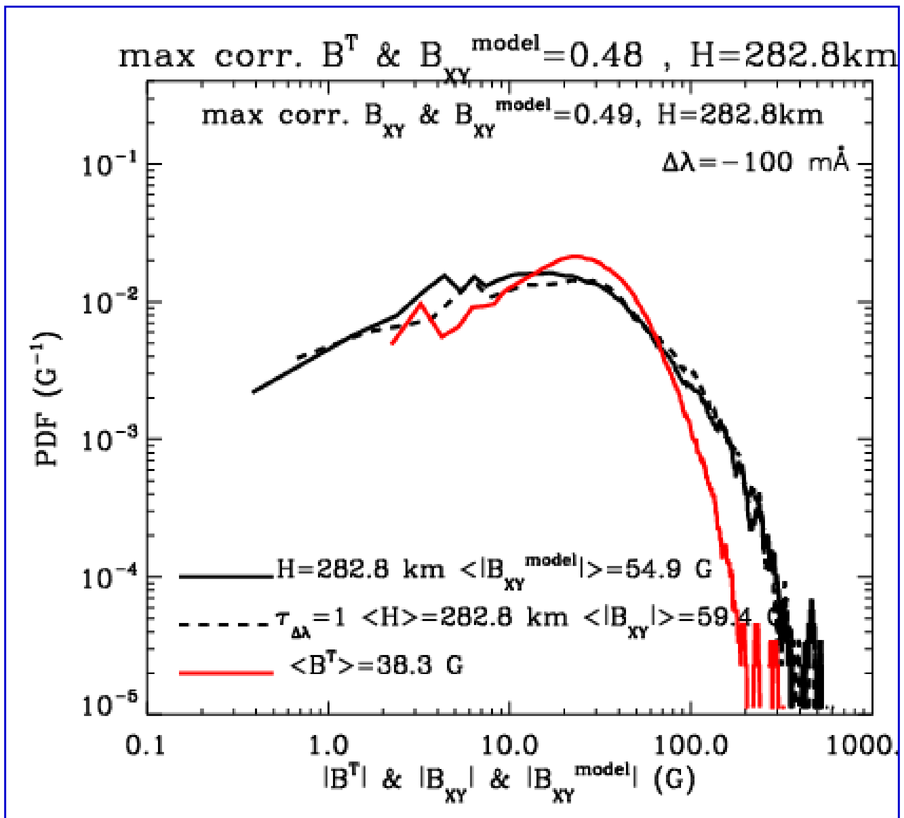

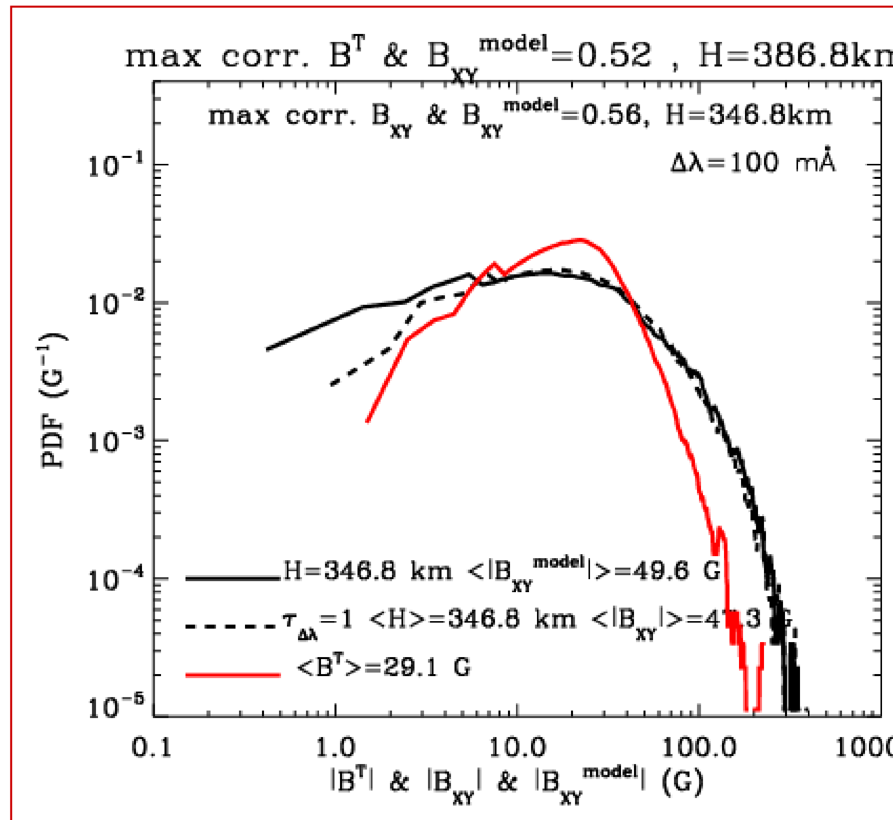

Mean “real” vertical and mean longitudinal magnetic fields VS mean height <H> of the layer

$$\tau_{\Delta\lambda} = 1$$

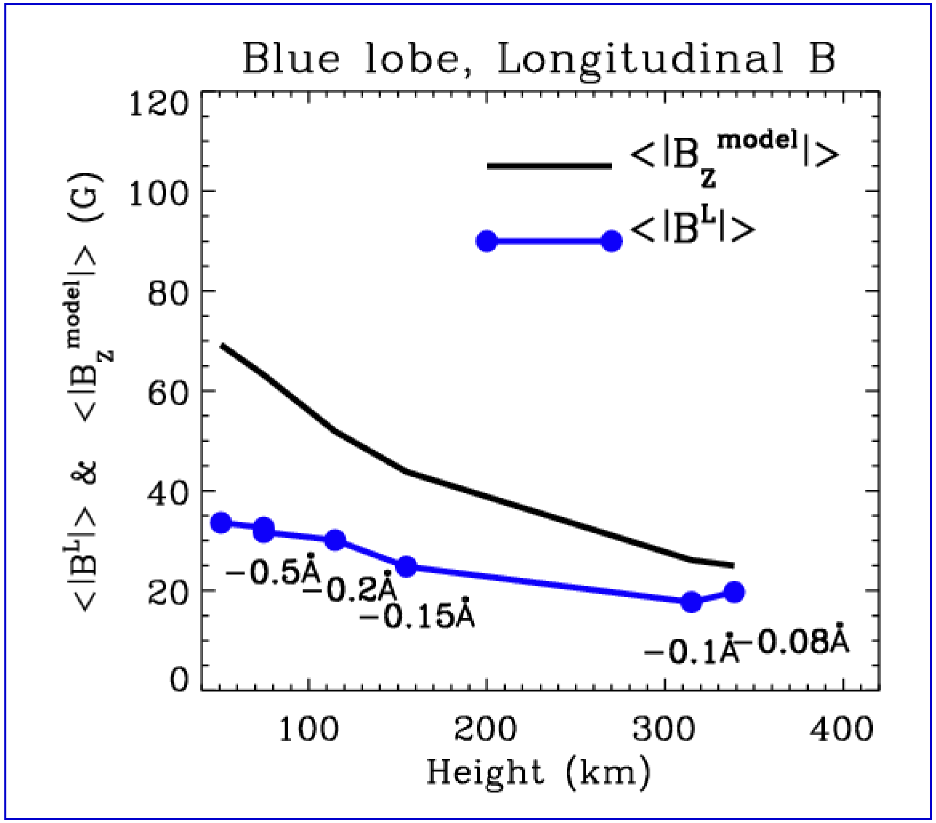

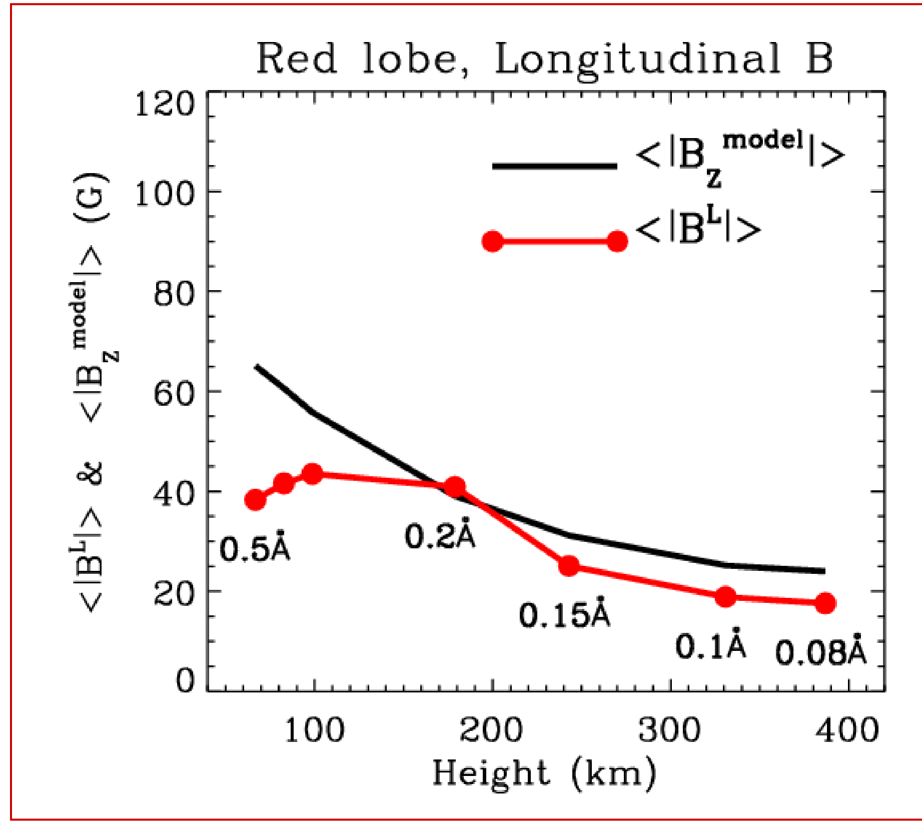

Longitudinal field (blue line) recovered from the blue wing

Longitudinal field (red line) recovered from the red wing

Mean “real” vertical (black line) and mean transverse magnetic fields VS mean height <H> of the layer

$$\tau_{\Delta\lambda} = 1$$

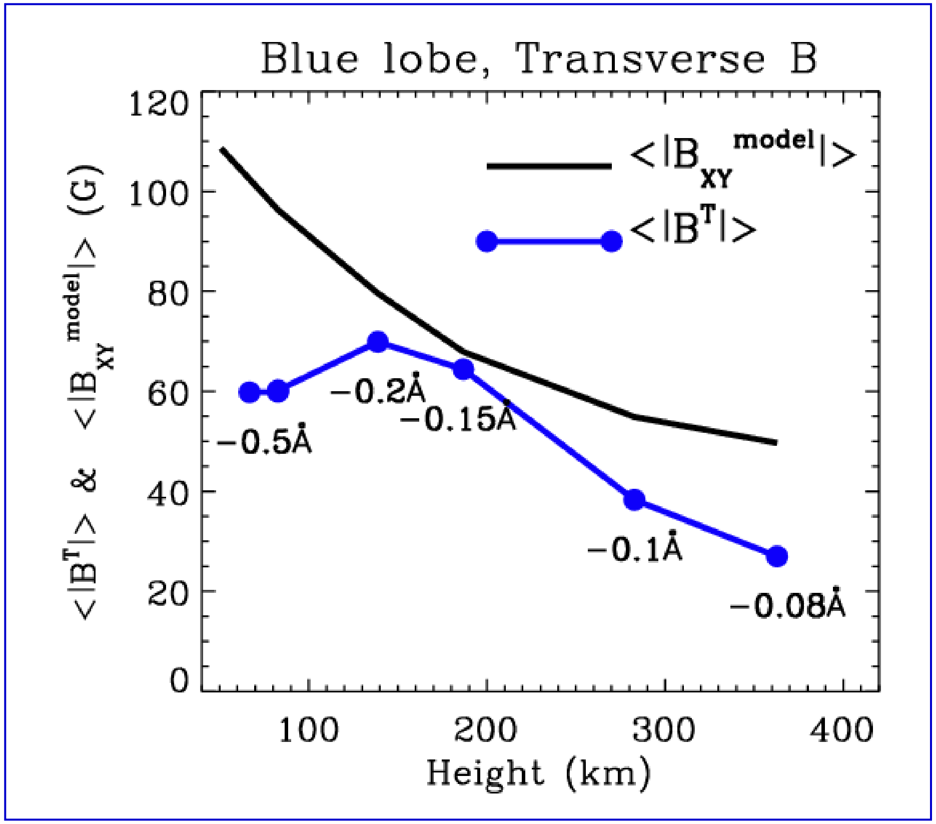

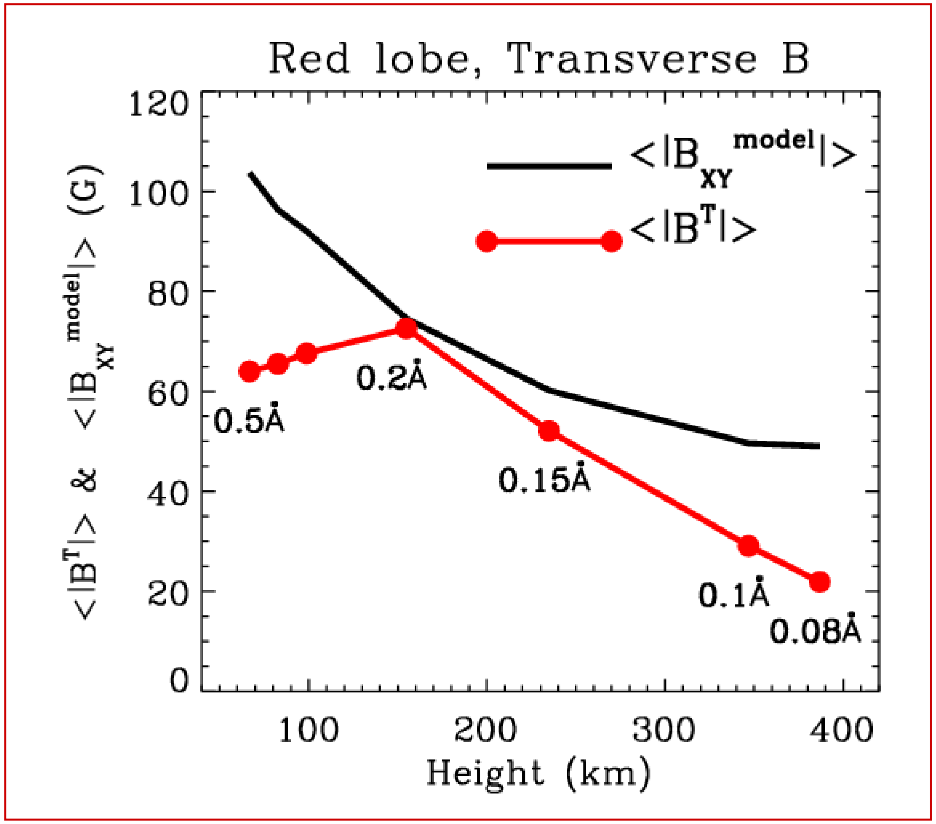

Transverse field (blue line) recovered from the blue wing

Transverse field (red line) recovered from the red wing

Concluding remarks

- The longitudinal & transversal components correlate remarkably well with spatial variations of the “real” vertical and horizontal components of the magnetic field strength taken at the surface $\tau_{\Delta\lambda} = 1$

- However, the mean longitudinal & transversal components are systematically smaller than the vertical & horizontal components taken at the surface $\tau_{\Delta\lambda} = 1$

- The peak of PDFs for B^T at around 10 G may be artifact due to underestimation of the “real” weak horizontal field.

- There are more abundant strong fields which we can not see using weak field approximation.

Spectropolarimetric diagnostics from the Hanle effect

Sr I 4607 Å

Multilevel radiative transfer modeling of the scattering polarization observed in the Sr I 4607 Å

- The solar 1D model using the free parameters (micro and macroturbulent velocities for line broadening)

See Faurobert-Scholl et al. 1993, 1995, 2001; Bommier et al. 2005;
Shchukina &Trujillo Bueno,2003,Solar Polarization 3,ASP Conf. Ser. 307, p.336

- The 3D surface convection (HD) model of Asplund, Nordlund & Stein (2000, A&A, 359, 729) with the microturbulent field having exponential distribution:

$$PDF(B)=Exp(-B/\langle B\rangle) / \langle B\rangle$$

See Trujillo Bueno, Shchukina & Asensio Ramos, 2004; Trujillo Bueno & Shchukina 2007

- The 3D MHD model with surface dynamo action of Vögler & Schüssler (2007, A&A, 465, L43).

See Shchukina & Trujillo Bueno, 2011

The Hanle-effect in Sr I 4607 Å line

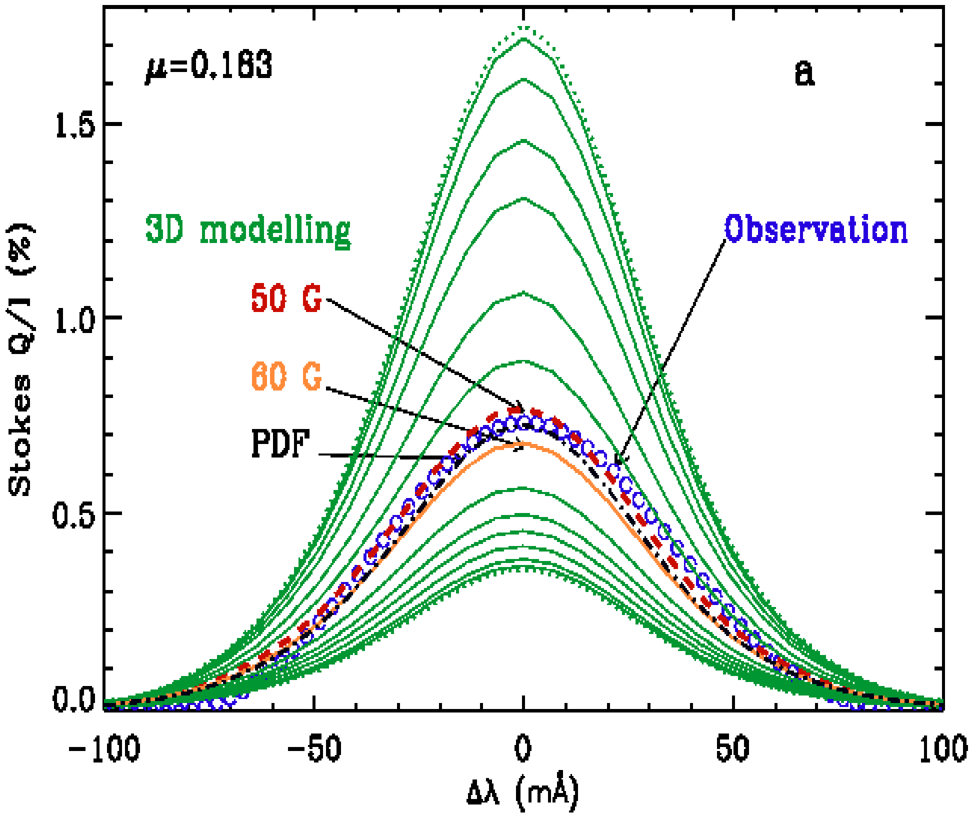

Hanle-effect modelling of the Sr I 460.7 nm line. The magnetic field produces a decrease in linear polarization for observations close to the solar limb.

Results

1D : $\langle B \rangle \approx 60$ G
3D MHD: $\langle B \rangle \approx 130$ G

- **The magnetic field is organized at the spatial scales of the solar granulation pattern, with relatively weak fields above the granules and with much stronger fields above the intergranular lanes.**

- **The average magnetic energy density:**

$$E = \langle B \rangle^2 / 8\pi = 1300 \text{ ergs/cm}^2$$

in the quiet solar photosphere is at least two orders of magnitude greater than that derived from simplistic 1D investigations.

- **The total magnetic energy stored in the inter-network regions is sufficient to balance radiative energy losses from the solar chromosphere.**

The surface variations of the Q/I & U/I amplitudes of Sr I 4607 Å line in the 3D local dynamo model (Vögler & Schüssler, 2007) with height-dependent scaling factor

1-m telescope smoothing
μ = 0.5

At the moment the Q/I profiles are observed with poor spatial and/or temporal resolution.

To detect and quantify the predicted surface fluctuations in Q/I & U/I signals would be important for our understanding the small-scale magnetic activity of the Sun.

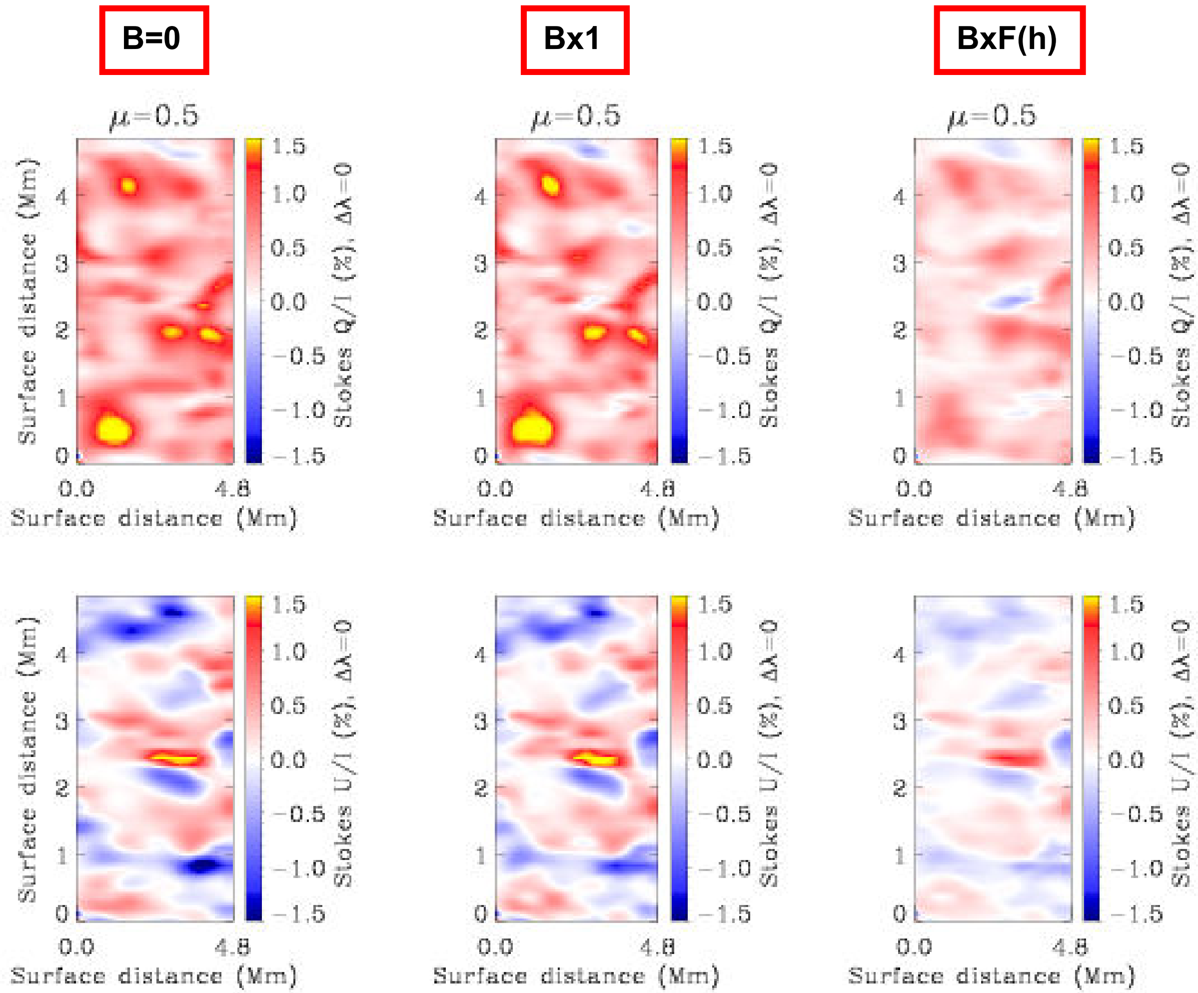

See details in Trujillo Bueno & Shchukina, 2007, ApJ, 664, L135

Shchukina & Trujillo Bueno, 2011, ApJ Letter, 731, L21

Thank you
for
your attention